Article

Current Biology

The atypical proteome of mitochondria from mature pollen grains

Graphical abstract

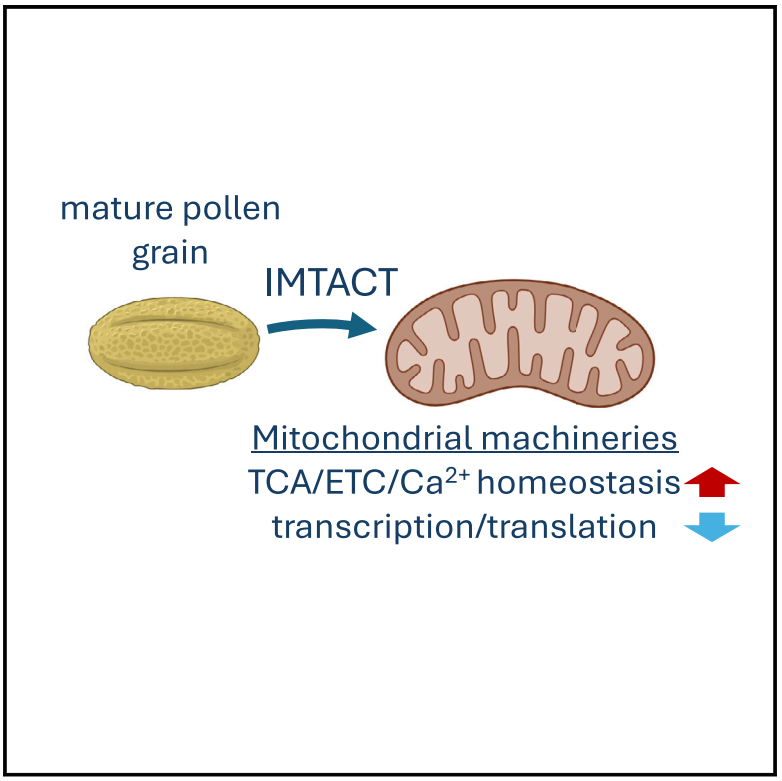

Authors

Clément Boussardon, Matthieu Simon, Chris Carrie, Matthew Fuszard, Etienne H. Meyer, Françoise Budar, Olivier Keech

Correspondence

etienne.meyer@pflanzenphys.uni-halle.de (E.H.M.), olivier.keech@umu.se (O.K.)

In brief

Boussardon et al. use the IMTACT method to successfully isolate mitochondria from mature pollen grains of Arabidopsis and show that these organelles have an atypical proteome highly depleted of proteins associated with transcription and translation machineries. This raises questions about the maintenance of respiratory functions during pollen germination.

Highlights

- IMTACT approach was successful in isolating mitochondria from mature pollen grains
- Pollen mitochondria accumulate proteins for TCA, ETC, and Ca^{2+} homeostasis
- Transcription and translation machineries are depleted in pollen mitochondria
- Maintenance of respiratory complexes is questioned

Boussardon et al., 2025, Current Biology *35*, 776–787
February 24, 2025
https://doi.org/10.1016/j.cub.2024.12.037

CellPress

CellPress
OPEN ACCESS

Current Biology

Article

The atypical proteome of mitochondria from mature pollen grains

Clément Boussardon,[1] Matthieu Simon,[2] Chris Carrie,[3] Matthew Fuszard,[4] Etienne H. Meyer,[5,*] Françoise Budar,[2] and Olivier Keech[1,6,*]

[1]Department of Plant Physiology, UPSC, Umeå University, 90187 Umeå, Sweden
[2]Université Paris-Saclay, INRAE, AgroParisTech, Institut Jean-Pierre Bourgin (IJPB), 78000 Versailles, France
[3]School of Biological Sciences, University of Auckland, 3 Symonds St., Auckland 1142, New Zealand
[4]Core Facility – Proteomic mass Spectrometry, Martin-Luther-University Halle-Wittenberg, Kurt-Mothes-Strasse 3a, 06120 Halle (Saale), Germany
[5]Department of Plant Physiology, Institute of Biology, Martin-Luther-University Halle-Wittenberg, Weinbergweg 10, 06120 Halle (Saale), Germany
[6]Lead contact
*Correspondence: etienne.meyer@pflanzenphys.uni-halle.de (E.H.M.), olivier.keech@umu.se (O.K.)
https://doi.org/10.1016/j.cub.2024.12.037

SUMMARY

To propagate their genetic material, flowering plants rely on the production of large amounts of pollen grains that are capable of germinating on a compatible stigma. Pollen germination and pollen tube growth are thought to be extremely energy-demanding processes. This raises the question of whether mitochondria from pollen grains are specifically tuned to support this developmental process. To address this question, we isolated mitochondria from both mature pollen and floral buds using the isolation of mitochondria tagged in specific cell-type (IMTACT) strategy and examined their respective proteomes. Strikingly, mitochondria from mature pollen grains have lost many proteins required for genome maintenance, gene expression, and translation. Conversely, a significant accumulation of proteins associated with the tricarboxylic acid (TCA) cycle, the electron transport chain (ETC), and Ca^{2+} homeostasis was observed. This supports the current model in which pollen requires large quantities of ATP for tube growth but also identifies an unexpected depletion of the gene expression machinery, aligned with the fact that the mitochondrial genome is actively degraded during pollen maturation. Altogether, our results uncover that mitochondria from mature pollen grains are strategically prepared for action by increasing their respiratory capacity and dismantling their gene expression machinery, which raises new questions about the assembly of respiratory complexes in pollen mitochondria, as they rely on the integration of proteins coded by the nuclear and mitochondrial genomes. In addition, the approach described here opens a new range of possibilities for studying mitochondria during pollen development and in pollen-specific mitochondrial events.

INTRODUCTION

Sexual reproduction in flowering plants relies on the production of large amounts of viable pollen grains. Pollen grains are the gametophyte individuals in Angiosperm species, which provide the link between two generations of diploid individuals by ensuring the protection and the dispersion of nuclear genes in the male lineage. They are considered to have played a key role in the spread and diversification of Angiosperms in land plant species.[1] Today, viable pollen is essential for the maintenance and propagation of germplasm collections that are widely used in plant breeding and agriculture.

Pollen grains are produced after meiosis from haploid microspores following a precise and complex developmental program.[2–4] The first part of this program starts just after meiosis: microspores undergo an initial mitotic division to generate generative and vegetative cells within the pollen grain. Subsequently, the generative cell undergoes a mitotic division to yield two sperm cells, i.e., the male gametes. This developmental phase is sustained by the sporophytic tapetal cells that cover the internal face of the anther locule and reaches its conclusion with the release of mature pollen grains from the anther. These grains are partially dehydrated, resistant capsules containing the two male gametes inside the companion vegetative cell. After deposition of a pollen grain on a compatible stigma, rehydration occurs, and the vegetative cell ensures the second part of its developmental program: it germinates out of the pollen wall and produces the growing pollen tube that enters the pistil and eventually delivers the two sperm cells into the embryo sac of an ovule.[3] It is now well established that proper mitochondrial functioning is crucial for both phases of pollen development, as witnessed by the sterilizing action of the coordinated expression of both nucleus- and mitochondrion-encoded genes causing cytoplasmic male sterilities.[5,6] Furthermore, the growth of the pollen tube requires a large amount of energy, which has been recently reported to be mainly provided by mitochondria.[7] Besides, while somatic cells possess between 40 and 400 copies of the mitochondrial genome, according to the cell type,[8]

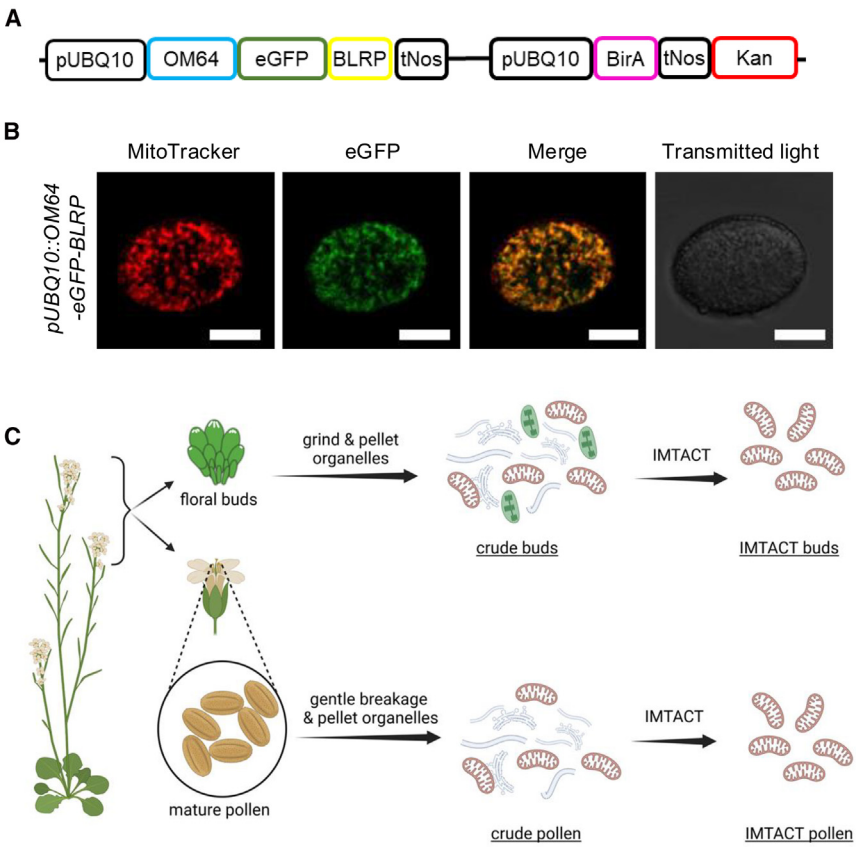

Figure 1. Pollen mitochondria isolation design and procedure

(A) One-shot IMTACT construct used for this study (see STAR Methods). *BirA* expression is driven by a constitutive *UBQ10* promoter. The *OM64* cDNA full-length form (*OM64*) was fused with *eGFP* and *BLRP*. The UBQ10 promoter allows the expression of *OM64* in mature pollen grain. The selection marker kanamycin was used here at the 3′ end of the construct. Details on the growth phenotype of T3 IMTACT plants in Figure S1.

(B) Fluorescence images of Arabidopsis mature pollen grain expressing the *OM64-eGFP-BLRP* fusion protein. Pollen grain from stable transformation lines was observed by confocal microscopy (40× magnification, water immersion), and co-localization was assessed using MitoTracker Orange. Scale bars, 10 μm. Confocal imaging of buds and pollen expressing (IMTACT) or not (WT) the OM64-eGFP-BLRP construct is shown in Figure S1C.

(C) Schematic representation of the procedure followed to obtain the diverse samples subjected to analysis (created with BioRender). Details about the isolation procedure in Figure S2.

approximately 130 copies of mitochondrial DNA per pollen grain were detected at the bicellular stage, and only 10 copies were found in mature pollen grains.[9] The limitation of mitochondrial DNA copy number in pollen at this late stage is likely linked to the control of maternal inheritance of the mitochondrial genome.[10,11] This is in line with the fact that mitochondrial DNA is actively degraded by specific endo- and exo-nucleases.[12,13] Moreover, mutants of mitochondrial proteins from various plant species show a defect in pollen formation.[14–17] Although these mutant plants are male sterile, their vegetative growth is generally not affected, and therefore they represent useful tools for plant breeding and hybrid formation. In addition, it is suspected that protective molecular mechanisms are in place to maintain the function of mitochondria in the dehydrated mature pollen. Taken together, these observations raise the question of the metabolic adjustments conferring the functional capacity of mature pollen mitochondria.

One way to address this question is to examine the mitochondrial proteome of mature pollen in detail. Although a few total proteomes of pollen grains have been analyzed for *Arabidopsis thaliana* and other flowering plants,[18–20] the technical limitations in the purification and analysis of pollen organelles have not yet permitted a focus on the mitochondrial compartment.[21]

In this study, we report the successful isolation of mitochondria purified from both mature pollen grains and floral buds, considered as a sporophytic reference. To achieve this, we utilized the isolation of mitochondria tagged in specific cell-type (IMTACT) strategy and adapted a previously described construct where the two expression cassettes necessary for the IMTACT procedure were placed under the control of the UBQ10 promoter (AT4G05320) to allow expression of the IMTACT proteins in the male gametophyte.[22,23] The UBQ10 promoter is ubiquitously active in Arabidopsis,[24] and transcripts from the UBQ10 gene were detected in developing pollen from the bicellular stage.[25,26] Taking advantage of this unprecedented ability to purify pollen mitochondria, we performed a comparative analysis of the proteomes of mitochondria isolated from mature pollen or buds. Our results show that mitochondria from mature pollen grains have lost their machinery for gene expression, DNA maintenance, and RNA maturation but instead have accumulated capacity for alternative pathways and energy production.

RESULTS

Purification of biotinylated mitochondria from floral buds and mature pollen

In a previous study, we generated T3 homozygous *Arabidopsis thaliana* Col-0 lines expressing the *OM64-eGFP-BLRP* and the *BirA* genes under the *UBQ10* promoter (Figure 1A).[22,23] No developmental difference was observed between these plants and their wild-type (WT) counterparts (Figure S1). To determine their suitability for pollen IMTACT experiments, mature pollen grains were assessed by confocal laser microscopy: the emission of the eGFP was confirmed in mature pollen and floral buds for lines expressing *OM64* under the control of the *UBQ10* promoter. Furthermore, eGFP colocalized with a MitoTracker (Figures 1B and S1). This confirms that the IMTACT construct is expressed and present in the two tissues of interest. This strategy allowed us to use the same line for the isolation of mitochondria from mature pollen and from floral buds, thus avoiding potential

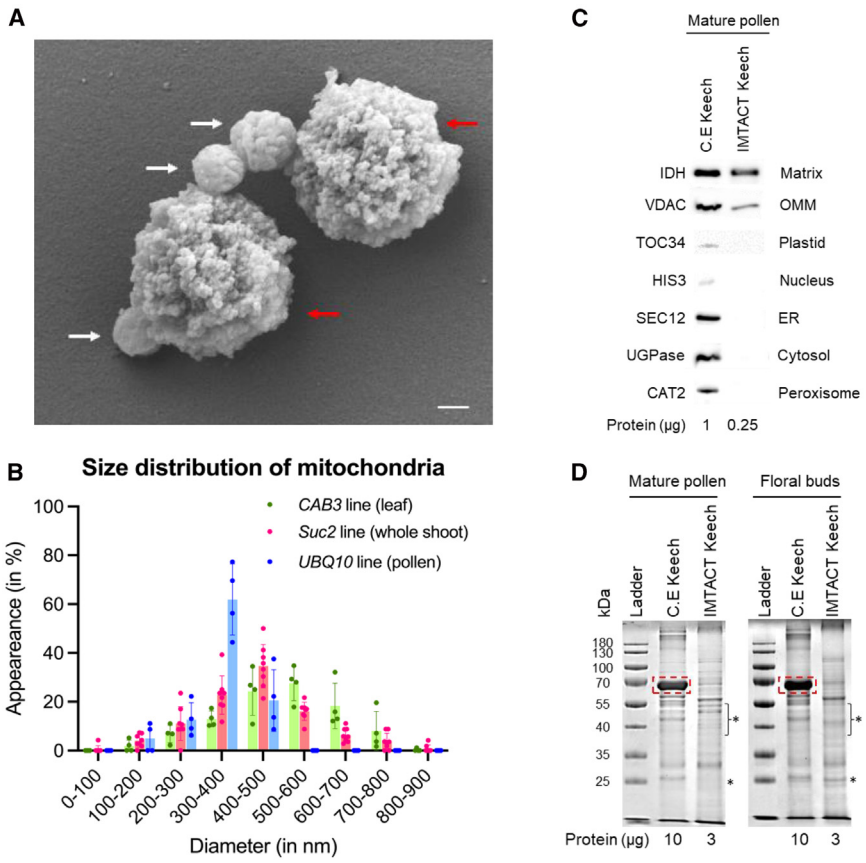

Figure 2. Quality control of pollen mitochondria isolated by IMTACT

(A) Scanning electron microscopy (SEM). A red arrow indicates a magnetic bead, while a white arrow points at a mitochondrion from pollen grains. Scale bar is 200 nm.

(B) Size distribution (in percentage) of the mitochondrial population isolated from mesophyll (4 replicates, $n = 176$), vascular (6 replicates, $n = 258$), and pollen (4 replicates, $n = 70$) cells. Mitochondrial size distribution for mesophyll and vascular cells was retrieved from Boussardon et al.[23]

(C) Enrichment and purity controls. Crude extract (CE) 1 μg and 250 ng of proteins obtained from purified mature pollen mitochondria were immunoblotted with anti-IDH (matrix) and anti-VDAC (outer membrane; OMM) to observe mitochondria enrichment. Anti-TOC34 (pollen) or LHCB (floral buds), anti-Histone3, anti-SEC12, anti-UGPase, and anti-CAT2 antibodies were used to check contamination by plastidial, nuclear, endoplasmic reticulum (ER), cytosolic, and peroxisomal proteins, respectively. The panel shows extracts obtained with buffers from Keech et al.[28] (see Figure S4 for entire gels and replicates).

(D) Total protein profile of mature pollen and floral buds mitochondria. CE 10 μg and 3 μg of proteins obtained from purified mitochondria were loaded on a 12% protein gel and stained by Coomassie. The panel shows extracts obtained with buffers from Keech et al.[28] Dashed red rectangles correspond to the BSA in the CE (66.5 kDa). (*) indicates obvious differences between the mitochondrial protein profiles after IMTACT. Estimation of pollen disruption efficiency and purity of mitochondria is shown in Figures S3 and S4, respectively.

discrepancies due to different integration sites of the IMTACT construct in the genome. Here, floral buds were considered as a sporophytic control since they mostly contain mitochondria from sporophytic tissues (i.e., receptacle, petals, sepals, carpels, stamens, and even the pistil to a large extent). Indeed, developing pollen grains are not broken during the isolation of mitochondria from the floral buds, and embryo sacs (i.e., female gametophyte) represent less than 300 cells in a whole bud (~ 40 × 7 cells).[27]

The experimental procedure for pollen collection and subsequent isolation of mitochondria using IMTACT is outlined in Figure 1C and detailed in Figure S2. In brief, approximately 6 g of inflorescences were collected from 20 plants per biological replicate. Mature pollen grains were released and purified, followed by breaking using a bead mill with approximately 50% of breaking efficiency (Figure S3). After pelleting the organelles in a crude extract, the IMTACT procedure thoroughly described in Boussardon and Keech[22] was conducted on both the pollen crude extract and the pellet obtained from whole floral buds (Figure 1C).

Scanning electron microscopy (SEM) was used to assess the interaction between mitochondria and beads in mature pollen samples. Consistent with previous observations with other constructs and samples,[23] 1 μm streptavidin beads were decorated with mitochondria exhibiting a predominantly spheroid shape (Figure 2A). Intriguingly, the vast majority of mitochondria isolated from mature pollen grains displayed diameters ranging between 200 and 500 nm, with ca. 60% of them falling in the 300–400 nm range (Figure 2B). This result contrasted with observations made in Boussardon et al.[23] for mitochondria isolated from mesophyll (*pCAB3*; 500–600 nm) and vascular tissues (*pSUC2*; 400–500 nm), indicating that mitochondria from mature pollen grains are smaller on average than those from mesophyll or vascular tissues.

Furthermore, a set of immunoblot controls was conducted to assess the efficiency of the IMTACT procedure. To this aim, 1 μg of crude extract and 0.25 μg of mitochondria isolated by IMTACT were loaded on a 12% acrylamide gel. A higher amount of protein in the crude extract was chosen to compensate for the large amount of bovine serum albumin (BSA) present in this sample. Representative proteins from the mitochondrial matrix and outer membrane, plastids, nucleus, endoplasmic reticulum, peroxisome, and cytosol were immunodetected to estimate the purity and integrity of the isolated mitochondria (Figures 2C and S4). Both matrix and outer membrane proteins were detected in the isolated mitochondria, supporting the fact that these mitochondria are intact. Hardly any non-mitochondrial proteins were detected at this stage, indicating very low contamination in the purified mitochondria. The total mitochondrial protein profile from mature pollen grains and floral buds was visualized by SDS-page (Figure 2D). Notably, differences were already evident at this level, underscoring the relevance of a detailed comparison between gametophytic (pollen) and sporophytic (buds) mitochondrial proteomes.

Production and global analyses of gametophytic and sporophytic mitochondrial proteomes

Proteomic analysis using liquid chromatography-tandem mass spectrometry (LC-MS/MS) was carried out on mitochondrial samples to determine the protein composition of mature pollen and floral buds tissues. To be able to evaluate enrichment in mitochondrial proteins, crude extracts were analyzed in parallel. A total of 4,250 protein groups were initially detected in at least one sample (intensity-based absolute quantification [iBAQ] values obtained from MaxQuant 2.1.3.0). Note that a protein group consists of several entries that cannot, based on the peptide and propensity score matching data, be distinguished. The dataset was subsequently filtered to retain only protein groups that were detected in at least 3 replicates of at least one of the four biological conditions (i.e., crude buds, crude pollen, IMTACT buds, or IMTACT pollen), resulting in a working dataset comprising 2,996 protein groups (iBAQ; Data S1A). The hierarchical clustering analysis clearly distinguished between the organs and grouped the replicates according to the condition (Figure S5A). A principal-component analysis (PCA) done from iBAQ data (Data S1A) shows that the extraction methods (crude or IMTACT) are mostly separated by component 1 (60%), and the tissue types (floral buds or pollen) are separated by component 2 (Figure S5B). Scatter plots, with Pearson correlation values of 0.6–1.0, indicate a good correlation between data obtained from the different replicates (Figure S5C; Data S1B). Therefore, the IMTACT treatment consistently impacted the protein content of the samples, and the mitochondrial proteomes from buds and pollen exhibited significant differences, confirming our observation from the Coomassie protein profiling (Figure 2D).

To further evaluate the efficiency of the IMTACT procedure, subcellular localization of the identified protein groups was predicted using the SUBA5 database.[29] Of the 2,996 protein groups of our working dataset, 771 were predicted to be mitochondrial proteins. This accounted for ca. 20% and 25% of proteins identified from the IMTACT with buds and pollen, respectively (Figure S6; Data S2). However, when considering the signal intensity of the protein groups, which is correlated to their abundance in the samples (Data S3), it was clear that mitochondrial proteins are enriched in IMTACT samples (Data S3A and S3B) compared with crude extracts (Data S3C and S3D): of the proteins with the highest signal intensity in pollen and floral buds IMTACT samples (percentile 90%), about 70% corresponded to mitochondrial proteins, while they represented 35% and 62% of the most abundant proteins in crude extracts of floral buds and pollen, respectively (Figure S7). This confirmed the efficiency of the IMTACT procedure, even though several contaminating proteins remained after purification. Also worth mentioning, the distribution of contaminants varied between the two tissues. While a strong proportion of cytosolic proteins were identified in pollen mitochondria, plastidial contaminants were mostly found in floral bud mitochondria (Figure S6; Data S1A).

Analysis of the peculiarities of mature pollen mitochondrial proteome

To further gain insight in this direction, label-free quantitation (LFQ) intensities were calculated from Data S1A using MaxQuant 2.1.3.0. The LFQ intensities calculation allowed normalization of protein intensities and provided the most accurate representation of ratio changes among different samples (Data S4A; $n = 1,819$). In this configuration, the replicates clustered well together, with tissue (component 1; 48%) and extraction (component 2; 25%) types better separated by PCA (Figure S8A; Data S4A). The number of identified differentially abundant protein groups (DAPs) between pollen and floral buds IMTACT datasets is shown in a volcano plot (Figure S8B; two-sided Student's t test, false discovery rate [FDR]: 0.05). Similarly to the iBAQ values (Data S1A), a strong correlation between LFQ replicates (values of 0.8–1.0) was evidenced (Figure S8C; Data S4B). To avoid compromising the biological relevance of the comparison between tissues, we decided to first prefilter our data through a "present/absent" step. This led to 671 "present" proteins in crude and 851 in IMTACT, while 1,148 and 968, respectively, were called as "absent." From the present dataset, we then applied a Student's t test with an FDR correction (at 0.05; Data S4A; Figures S8D and S8E). Similarly to the full Data S4B (Figure S8C), a strong correlation between LFQ replicates was observed (Figure S8E).

The working dataset was then filtered to focus on mitochondrial proteins, and both shared and specific protein groups in each tissue were assessed (Figure S9; Data S4A). A total of 252 protein groups were found in all samples. While no protein groups were exclusive to crude samples, 54 and 19 were specific to the IMTACT bud and pollen mitochondria, respectively. In line with our previous observations, we hypothesized that the different protein composition between pollen and floral bud mitochondria revealed by our observations reflects specificities in the mitochondrial functions of pollen.

We established a biological network based on enriched Gene Ontology (GO) terms using Cytoscape[30] and the ClueGO plugin.[31] Enriched GO terms associated with mitochondrial proteins significantly more or less abundant (Student's t test; $p < 0.05$) in mature pollen than in floral buds were clustered according to their functional categories (Figure 3A; Data S5A; details about clustering in Data S5B). Translation, tRNA modifications, gene expression, and metabolic regulations for several amino acids were among the most prominent GO terms in mitochondrial proteins that were more abundant in floral buds. Conversely, the most significantly enriched GO terms in mitochondrial proteins that are more abundant in mature pollen were tricarboxylic acid (TCA) cycle, cellular respiration, nucleotide metabolic process, and respiratory electron transport chain (ETC).

Subsequently, mitochondrial proteins were functionally categorized according to the latest iteration of MapMan,[32] and the distribution of differentially abundant proteins was compared between bud and pollen IMTACT samples (Figure 3B; Data S4A and S6). Of the 571 proteins, 183 did not show any significant difference between samples, while 252 and 136 DAPs were found to be accumulated to a greater degree in floral buds and pollen IMTACT samples, respectively. Half of the identified DAPs that accumulated to a greater abundance in floral buds were associated with RNA metabolism (RNA category) and translation (protein category). By contrast, 35% of the 136 DAPs, which were found to be more abundant in pollen, were related to the ETC and TCA. This overview clearly indicates that mitochondria from mature pollen are different from bud mitochondria, as proteins involved in gene expression and translational activity are depleted but potentially contain a higher capacity to support energy metabolism.

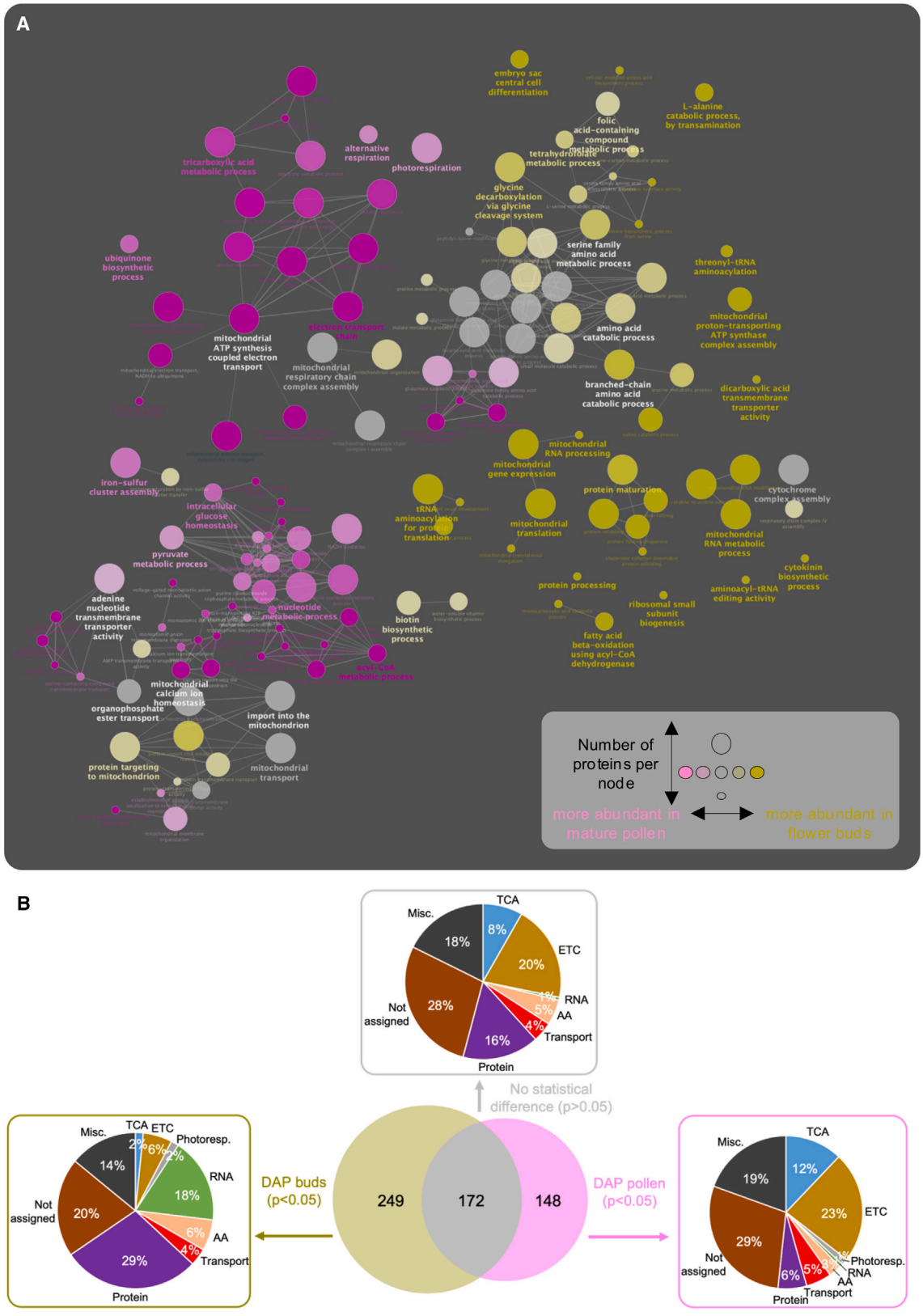

(legend on next page)

Pollen mitochondria are strongly depleted of ribosomal and RNA metabolism proteins

Finally, to provide an accurate representation of the biological functions concerned by such differential protein abundances between pollen and sporophytic mitochondria, Bins (root nodes) were divided into sub-Bins (intermediate nodes) (Data S6; n = 388). Strikingly, within Bin 29, which encompasses 77 protein groups associated with proteins/translation, 49 protein groups were not detected in pollen, and an additional 18 were less abundant in the pollen samples. Of these, 36 mitochondrial ribosomal proteins were not detected in pollen samples (Figure 4A). Additionally, 7 tRNA ligases and 4 folding proteins (including chaperones and heat-shock proteins) were also found in lower abundances in mitochondria from pollen. Similarly, RNA-binding proteins involved in gene expression, such as pentatrico peptide repeat (PPR) proteins, were scarcely detected in pollen samples (Bin 27; Figure 4B). In this category, many protein groups were found in bud mitochondria, including eight uncharacterized proteins, PRECOCIOUS1 (associated with flowering time), nine ribosomal (RPPR2, RPPR3A, RPPR3B, RPPR4, RPPR5, RPPR7, RPPR8, DWEORG1, and MS80), one splicing (BIR6), one maturation (mTERF6), and four RNA editing (PPR596, GRP23, NUWA, and DYW2) PPR proteins. None of these were detected in pollen mitochondria. In addition, other protein groups (non-PPRs) that play a significant role in processing the numerous RNA-editing sites found in the mitochondrial transcriptome were also underrepresented in the mature pollen mitoproteome. For example, the class of multiple organellar RNA-editing factors (MORFs) constitutes a small family of proteins targeted to organelles, and notably, five proteins within this family were not detected in mitochondria from pollen tissues in contrast to the sporophytic samples. Furthermore, 10 proteins involved in transcription regulation and 5 RNA-binding glycine-rich proteins (RBGA1, 2, 4, 5, and 7) associated to RNA metabolism were mostly not found or significantly decreased in abundance in pollen. Taken together, these findings confirm that expression of the mitochondrial genome, including transcription, transcript maturation, and translation, is either significantly impaired or absent in mitochondria from mature pollen grains.

Pollen mitochondria are rich in proteins involved in energy production

In contrast to the expression of the mitochondrial genome, protein groups associated with both the TCA and ETC metabolic functions were significantly more abundant in pollen, with only a few exceptions. One isoform of isocitrate dehydrogenase (IDH-II), a pyruvate dehydrogenase E3, and two NAD-dependent malic enzymes (NAD-ME) were found in higher abundances in buds (Figure 4C; Figure S10). On the other hand, differentially abundant complex I (NADH dehydrogenase) subunits were spread over the two samples, with 8 proteins less abundant and 8 more abundant in pollen as compared with the floral buds, which thus does not provide any clear indication regarding the abundance of complex I in these mitochondria (Figure 4D). Of note, two prohibitins that were less abundant in pollen were associated with complex I by MapMan, although their involvement in OXPHOS has not been experimentally confirmed. Four Ca^{2+}-dependent type II NADH dehydrogenases proteins (NDA2, NDB2, and NDB3) and two succinate dehydrogenase assembly factors were more abundant in pollen compared with buds. Similarly, one isoform of alternative oxidase (AOX1b), one ubiquinol:cytochrome *c* oxidoreductase complex III protein (CYC1-1), one cytochrome *c* isoform (CYTC-2), six cytochrome *c* oxidase (complex IV) subunits, and five ATP synthase (complex V) proteins were all significantly more abundant in mitochondria from mature pollen grains. In addition, two ADP/ATP carriers (AAC1 and AAC2), involved in ATP export from the matrix, were more abundant in pollen mitochondria. This validates the idea that the main role of mitochondria in pollen is to provide the ATP required for the rapid growth of the pollen tube.

Other specificities of the pollen mitochondria proteome

Examining transporters, this proteome analysis revealed that several mitochondrial Ca^{2+} uptake IMM transporters (mitochondrial calcium uptake 1 and 2 [MCU1, MCU2] and the mitochondrial Ca^{2+} uniporter MICU), as well as one voltage-dependent anion channel OMM transporter (VDAC2), were significantly upregulated in mitochondria from pollen (Figure S11). VDACs are encoded by a gene family of five outer membrane transporters, mostly involved in metabolite exchange between the cytosol and the intermembrane space. This suggests the biological significance of a calcium influx in mature pollen. The coenzyme A transporter (COAC1) was found to be more abundant in pollen, whereas a few other transporters for NAD (NDT2), protons (UCP3), Mg-ATP^{2}F02D (APC1), and pyruvate (mitochondrial pyruvate carrier 1 [MPC1]) were less abundant (Figure S11). Among the protein groups with no assigned functional category, three proteins known to interact with mtDNA (GYRA, SWIB6, and

Figure 3. Gene Ontology network

(A) Biological network of enriched GO terms (biological process; Data S5) from significantly (Student's t test; FDR, $p < 0.05$) differentially abundant proteins in mitochondria from mature pollen versus mitochondria from flower buds in Data S4 (LFQ values; n = 1,819). Enriched GO terms upregulated in mitochondrial proteomes from mature pollen (palette of pink) or downregulated (palette of beige) were clustered according to their functional categories. The size of a node is proportional to the number of proteins contributing to this node, while the intensity of the color is proportional to the significance of it (the minimum for significance being $p < 0.05$); gray nodes = overrepresented in the protein subset but not enriched significantly; and the threshold of significance was set at 60% (see STAR Methods). Details about the analysis of the iBAQ datatset (Data S1) in Figure S5.

(B) Charts representing differentially abundant proteins (DAP) extracted from MapMan in buds and pollen IMTACT samples from Data S4 (LFQ values). The Venn diagram shows proteins not differentially accumulated (n = 183) or more abundant in buds (n = 252) or pollen (n = 136). Pie charts represent details of functional categories of significantly more abundant proteins detected by mass spectrometry (MS) in pollen or buds. Statistics: Student's t test (FDR $p < 0.05$; two-tailed distribution). Bins 1 (photorespiration), 2 (CHO metabolism), 8 (TCA), 9 (ETC), 10 (cell wall), 11 (lipid metabolism), 12 (N-metabolism), 13 (amino acid metabolism), 16 (secondary metabolism), 18 (cofactor and vitamin metabolism), 20 (stress), 21 (redox), 23 (nucleotide metabolism), 25 (C1 metabolism), 26 (miscellaneous), 27 (RNA metabolism), 29 (protein), 30 (signaling), 31 (cell division), 34 (transport), and 35 (not assigned) were extracted. Bins 2, 10, 11, 12, 16, 18, 20, 21, 23, 25, 26, 30, and 31 were grouped in the miscellaneous (Misc.) category.

See also Data S1, S2, S3, and S4.

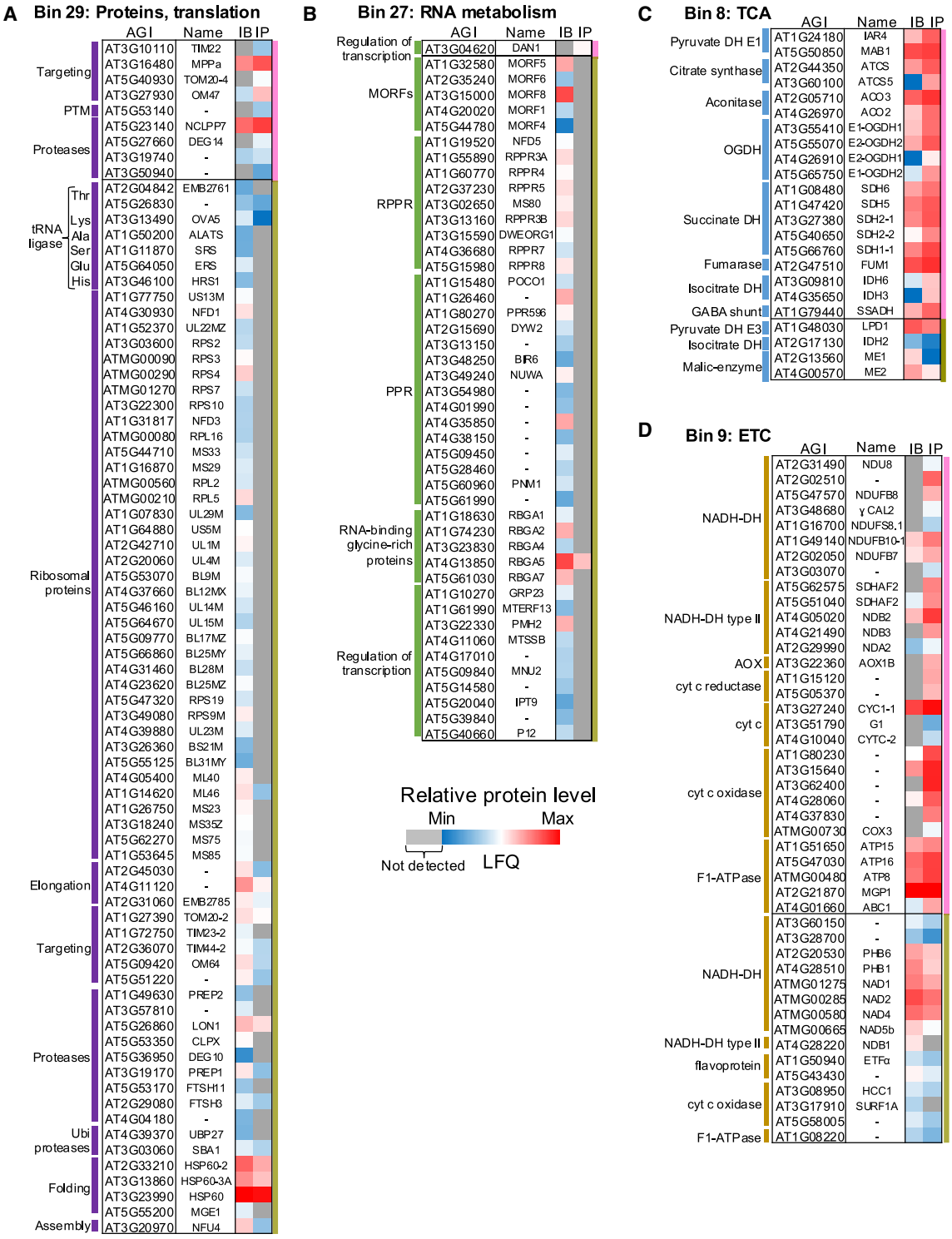

Figure 4. TCA, ETC, and gene expression-related DAPs detected by MS

Heatmaps represent the detail of DAPs (Student's t test; FDR $p < 0.05$) in buds (IB) and pollen (IP) after IMTACT (for corresponding gene description, see Data S4; LFQ intensities). Colored bars on the right of the heatmaps: significantly more abundant in pollen (pink) or in buds (beige). Categories were isolated from LFQ transformation, averaging, and filtering ($n = 388$). Details about the subcellular localization analysis in Figures S6 and S7. Analysis of the LFQ filter dataset (Data S4A) is detailed in Figures S8 and S9.

(A–D) (A) Protein metabolism/translation (Bin29; $n = 77$), (B) RNA metabolism (Bin27; $n = 45$), (C) TCA (Bin8; $n = 23$), and (D) ETC (Bin9; $n = 45$). Details on the TCA cycle are shown in Figure S10. Photorespiration, AA metabolism, transport, miscellaneous, and not assigned-related DAPs detected by MS are shown in Figures S11 and S12 and Data S6. In blue: the lowest protein level in a defined functional category. In red: the highest protein level in a defined functional category.

(legend continued on next page)

WHY2) were absent from pollen samples (Figure S12), supporting the idea of low mitogenome content. Interestingly, the third most abundant pollen protein was a LEA protein (Data S4A), a member of a family of proteins that are expressed during seed maturation and play roles in the protection of membranes during dehydration. This indicates that, during pollen maturation, the mitochondrial proteome is adapted to prevent damage resulting from the programmed dehydration.

Change in protein composition results from a transcriptional reprogramming

The analysis of the pollen mitochondria proteome shows that many protein groups are depleted. To evaluate the origin of this response, we queried a published RNA sequencing (RNA-seq) dataset (accession code E-MTAB-9456, ArrayExpress) investigating changes in gene expression during pollen development[19] and extracted transcript abundance data for all the mitochondrial proteins we identified in our study. This analysis evidenced that transcripts encoding for mitochondrial proteins that were not detected in pollen are depleted between the binucleate and trinucleate stage (Figure S13). The corresponding proteins would be expected to be depleted more or less rapidly depending on their half-life. Mitochondrial proteins involved in DNA/RNA metabolism or protein synthesis were found to have a relatively short half-life in cell cultures.[33] By contrast, transcripts encoding proteins identified in mature pollen were still detectable in the trinucleate stage. Altogether, this suggests that the expression of many genes encoding mitochondrial proteins is repressed during pollen development.

DISCUSSION

Here, we report the production of a mitoproteome from Arabidopsis mature pollen grains by implementing the IMTACT method. The major obstacle to obtaining a mitoproteome from Arabidopsis pollen was the mechanical resistance of pollen grains, whose walls are known to resist thousands of years in the soil.[34] The main challenge was to liberate intact mitochondria from the pollen wall armor. We could successfully apply the IMTACT procedure on the extracts only after optimization of the method used to release the cytoplasmic content from mature pollen grains while minimizing a physical alteration of mitochondria.

Mitochondrial proteins were more abundant in our pollen crude samples than in those from floral buds, which is consistent with the well-documented high mitochondrial density in pollen grains: for instance, it has been estimated that pollen contain 20 times more mitochondria per cell than vegetative tissues in *Zea mays*.[35] After the IMTACT procedure, purified mitochondria samples were deemed suitable for proteomic analysis by both electron microscopy and immunoblot analyses. Although contaminants were scarcely detectable by western blot, only 20%–25% of the identified protein groups were predicted to be mitochondrial, yet these mitochondrial proteins accounted for more than 70% of the total amount of proteins in the samples, therefore confirming a substantial enrichment (Figures S6 and S7). It is conceivable that, in mature pollen, cellular compartments must contend with spatial constraints imposed by dehydration[36]: the biotin labeling is more likely to affect other compartments, which subsequently can increase contaminants. The dehydrated state of mature pollen may also explain the small size of mature pollen mitochondria as compared with their counterparts extracted from floral buds (Figure 2B). This approach allowed for the detailed comparison of the mitochondrial proteomes from mature pollen and floral buds, which offers an unprecedented view of the unique functional status of mature pollen mitochondria (Figure 5).

One remarkable feature of mature pollen is their drastically low amount of mitochondrial DNA, despite the large number of organelles (see introduction). Furthermore, a genetically induced increase in pollen mitochondrial DNA copy number at the late stages resulted in anomalies in respiration and pollen tube growth.[9] This suggests that the limitation of mitochondrial DNA copy number in mature pollen grains has a significant physiological role for successful reproduction. The Arabidopsis mitochondrial genome encodes 33 mRNAs that are translated in the organelle. Hence, complete transcriptional and translational machineries are required for the production of mitochondrion-encoded proteins, which are major components of the ETC complexes and mandatory elements for the production and assembly of these complexes (ribosomal proteins and assembly factors). Yet, most members of mitochondrial gene expression machineries are encoded by the nucleus, produced in the cytosol, and imported into mitochondria for assembly and function. Our analysis showed that many proteins required for gene expression and translation were dramatically underrepresented or even not detected in mature pollen grains. This result is coherent with the depletion of transcripts encoding these proteins at the tricellular pollen stage (Figure S13). It implies that the few copies of the mitochondrial genes that remain in mature pollen cannot be used for providing new functional subunits to ETC complexes.

Indeed, pollen germination and tube growth require a highly active energy metabolism, and mitochondria were shown to be the major supplier of cytosolic ATP during pollen tube growth.[7] However, mitochondrial energy metabolism in the pollen tube remains to be thoroughly investigated, in particular considering the restrictive oxygen conditions in the pistil transmitting tract.[37,38] With that being said, it has recently been proposed that fermentation is not essential for pollen tube growth in Arabidopsis.[7] Our results enlighten the energy-producing capacity of Arabidopsis pollen mitochondria at the start of its rehydration on a compatible stigma. We observed that 17 TCA enzymes over-accumulated in pollen compared with sporophytic tissues of the buds. It is also the case of the coenzyme A (CoA) inner membrane transporter, COAC1, and of pollen-specific ALDH2B7 protein,[7] which functions as an aldehyde dehydrogenase facilitating the conversion of acetaldehyde—which is transported from the cytosol—to acetate. Acetate and CoA are utilized by the acetyl CoA synthetase (ACS) to produce acetyl CoA, which then feeds the TCA cycle.

In gray: proteins not detected by MS in any of the four replicates. AOX, alternative oxidase; cyt *c*, cytochrome *c*; DH, dehydrogenase; Misc., miscellaneous; MORFs, multiple organellar RNA editing factor; N.d., not detected; OGDH, 2-oxoglutarate dehydrogenase; PPR, pentatricopeptide repeat; PTM, post-translational modification; RPPR, ribosomal PPR; Ubi, ubiquitin.
See also Data S4 and S6.

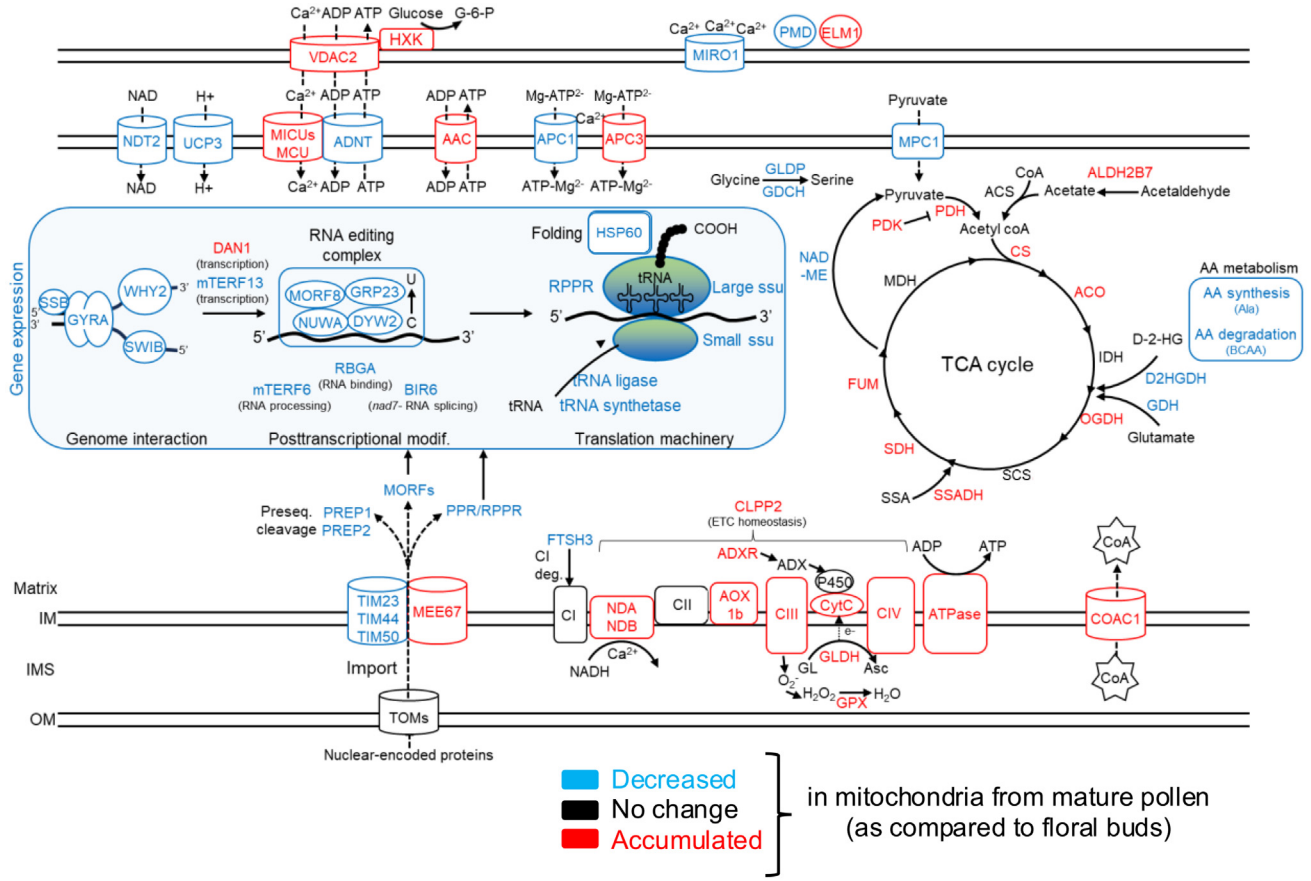

Figure 5. Working model comparing mature pollen and floral bud mitochondria

In mature pollen grains, mitochondria accumulate Ca^{2+} and CoA transporters to feed energy metabolism pathways. TCA and ETC proteins globally accumulate in mature pollen, enhancing the production of redox cofactors and ATP. The ATP produced is then used for pollen germination. On the other hand, proteins belonging to transcriptional, post-transcriptional, translational, and post-translational machineries (named "gene expression") strongly decreased in mature pollen. Those machineries could almost be arrested, as most of the proteins present in buds are not detected in pollen. RNA-seq data for TCA, OXPHOS, RNA metabolism, and protein synthesis during pollen development were obtained from Klodova et al.[19] and are shown in Figure S13. In blue: proteins more accumulated in buds. In black: proteins evenly accumulated. In red: proteins more accumulated in pollen grains. Dashed arrows: import. In gray: unclear function in plants. All data found in Data S4.

AAC, mitochondrial ADP/ATP carrier; ACO, aconitase; ACS, acetyl CoA synthetase; ADNT, adenine nucleotide transporter; ADX, adrenodoxin; ADXR, adrenodoxin reductase; ALDH2B7, aldehyde dehydrogenase 2B7; AOX1b, alternative oxidase 1b; APC, ATP/phosphate carrier; BIR6, buthionine sulfoximine-insensitive roots 6; CI, complex I; CII, complex II; CIII, complex III; CIV, complex IV; CLPP2, caseinolytic protease 2; COAC1, CoA carrier 1; CS, citrate synthase; D-2-HG, d-2-hydroxyglutarate; D2HGDH, D-2-hydroxyglutarate dehydrogenase; ELM1, elongated mitochondria 1; FTSH3, FTSH protease 3; FUM, fumarase; G-6-P, glucose-6-phosphate; GDCH, glycine decarboxylase complex H; GDH, glutamate dehydrogenase; GLDH, L-galactono-1,4-lactone dehydrogenase; GLDP, glycine decarboxylase P-protein; GPX, glutathione peroxidase; GRP23, glutamine-rich protein 23; GYRA, gyrase A; HSP60, heat-shock protein 60; HXK, hexokinase; IDH, isocitrate dehydrogenase; MCU, mitochondrial calcium uptake; MDH, malate dehydrogenase; MICU, mitochondrial calcium uptake protein; MIRO1, MIRO-related GTPase 1; MORF, multiple organellar RNA editing factor; MPC1, mitochondrial pyruvate carrier 1; mTERF, mitochondrial transcription termination factor; NAD-ME, NAD-dependent malic enzyme; NDA, alternative NAD(P)H dehydrogenase A; NDB, NAD(P)H dehydrogenase B; NDT2, NAD^+ transporter 2; NUWA, alias embryo defective 1,796; OGDH, oxoglutarate dehydrogenase; P450, cytochrome P450; PDH, pyruvate dehydrogenase; PDK, pyruvate dehydrogenase kinase; PMD, peroxisomal and mitochondrial division factor; PPR, pentatricopeptide repeat; PREP, pre-sequence protease; RBGA, RNA-binding glycine-rich protein A; RPPR, ribosomal pentatricopeptide repeat; SCS, succinyl-CoA synthetase; SDH, succinate dehydrogenase; SSA, succinic semialdehyde; SSADH, succinic semialdehyde dehydrogenase; SSB, single-stranded DNA-binding protein; SWIB, swi/snf protein complex B protein; TIM, translocase of the inner membrane; TOM, translocase of the outer membrane; UCP, uncoupling protein; VDAC2, voltage-dependent anion channel 2; WHY2, WHIRLY 2.

See also Data S5.

These observations suggest that mature pollen grains retain a strong capacity to produce NADH, $FADH_2$, and ATP from the TCA cycle as soon as rehydration occurs.

NADH and $FADH_2$ are substrates for complexes I and II of the ETC, respectively. Complex I is the main entrance point of electrons into the ETC, transferring them from NADH to ubiquinone. Ten subunits of complex I accumulated in pollen while eight members increased in floral buds (Figure 4D). As almost one-quarter of the mitochondrial genes encode products important for complex I biogenesis, it is not surprising to detect

ambiguous protein levels for this complex. The mitochondrion-encoded subunits (Nad1, Nad2, Nad4, and Nad5) were all found to be less increased in pollen than in buds (Figure 4D), consistent with the impaired mitochondrial gene expression observed in pollen. On the other hand, the alternative NADH-ubiquinone dehydrogenases NDA2, NDB2, and NDB3 were predominant in pollen, whereas only NDB1 accumulated in floral buds. Complex III transfers electrons from the ubiquinol to cyt *c*. Electrons from cyt *c* are transferred to oxygen by complex IV. The electron flow creates a proton gradient across the inner membrane, allowing complex V to produce ATP. Several components of these complexes accumulated in pollen (Figure 4D). Of note, the CLPP2 protein, which contributes to the coordination and homeostasis of the ETC,[39] was more abundant in mature pollen than in floral buds. This protein may thus be relevant in the context of an impeded production of mitochondrion-encoded subunits for the ETC complexes. Overall, we propose that the increased abundances observed for NDA2, NDB2, and NDB3 potentially favors electron entrance through external type II dehydrogenases. The electron flow is facilitated by a global accumulation in subunits of complexes III and IV, and an enhanced proton motive force along with the accumulation of complex V subunits allows for increased ATP production in pollen. It is also worth highlighting that only one isoform of the AOX1b was detected only in mitochondria from pollen. Taken together with the presence of external dehydrogenases, this suggests a strong capacity for the alternative pathway in mitochondria from pollen. Whether this plays a physiological role in limiting ROS production or buffering the redox state during pollen tube development remains to be investigated.

Our results also indicate that the control of Ca^{2+} flux/pool is a major function for which the mitoproteome of mature pollen grains is particularly well equipped. Indeed, Ca^{2+} distribution, modulation, and flux were shown to play major roles in pollen tube germination, interaction with female tissues, tip growth, and delivery of sperm cells.[40,41] Mitochondria are likely important contributors in the management of Ca^{2+} pools and fluxes in the vegetative cell during pollen tube growth. Indeed, the mitochondrial Ca^{2+} uniporter complexes were shown to be essential for pollen tube germination and growth.[42] The accumulation of VDAC2, MCU1, MCU2, and MICU in pollen mitochondria as compared with floral buds suggests a higher capacity for modulating their Ca^{2+} pool. MICU is a mitochondrial uniporter playing a key role in Ca^{2+} homeostasis. Mutants of MICU exhibit altered mitochondrial calcium levels but do not display any observable macroscopic phenotype. It has been suggested that MICU plays a role in conferring tolerance to high Ca^{2+} stress.[43,44] Interestingly, based on the study of a *micu* knockout mutant, it was recently proposed that Ca^{2+} signaling may also influence the TCA cycle and amino acid production.[45] This is in line with previous studies suggesting that once in the intermembrane space and matrix of mitochondria, Ca^{2+} promotes TCA activity and increases NADH levels through its interaction with dehydrogenases in mammalian cells.[46,47] Furthermore, an increase in the outer membrane Ca^{2+} sensing adaptor protein MIRO1 was observed. In plants, the *miro1* mutant exhibits a pronounced phenotype, characterized by impaired pollen germination and tube growth.[48] Altogether, these results support a model where pollen mitochondria are equipped for fluctuating Ca^{2+} fluxes, which is in line with earlier studies reporting a significant Ca^{2+} gradient in the developing pollen tube.[40,49] Whether this modulation in Ca^{2+} levels subsequently influences mitochondrial metabolism in such a way that it becomes physiologically relevant for the pollen tube germination and growth remains, however, to be investigated.

To conclude, we report a compelling example of plant mitochondria with a dramatically altered composition. Mitochondria of Arabidopsis mature pollen are equipped with the proteome necessary for their ''kamikaze'' mission of sustaining germination and growth of the pollen tube, without hope of transmitting their genome to the next generation. In particular, our results show that mature pollen mitochondrial proteome is fine-tuned to provide an adequate capacity for energy production and Ca^{2+} homeostasis required for the reproduction phase. The low mitochondrial DNA copy number could appear coherent with the extremely low amount, if any, of the machinery for mitochondrial gene expression we observed. Yet, this result raises the question of the turnover of mitochondrion-encoded proteins for the ETC: is the mitochondrial DNA expressed during pollen tube growth? Analysis of the mitoproteome of germinating pollen, for example, implementing the IMTACT approach using a late pollen promoter (such as LAT52[50,51]), will be instrumental to address this question. Such analysis would provide a better understanding of the mitochondrial contribution to the pollen tube energy metabolism as well as paving the way to the exploration of pollen-specific events in which mitochondria play a major role.

RESOURCE AVAILABILITY

Lead contact

Further information and requests for resources and reagents should be directed to and will be fulfilled by the lead contact, Olivier Keech (olivier.keech@umu.se).

Materials availability

Arabidopsis line (T3) containing the *UBQ10::OM64-eGFP-BLRP* and *UBQ10::-BirA* IMTACT construct used in this study can be obtained from the lead contact upon request.

Data and code availability

All data reported in this paper will be shared by the lead contact upon request. Mass spectrometry proteomics data is publicly available on the ProteomeXchange Consortium via the PRIDE partner repository with the dataset identifier PXD050553 (https://www.proteomexchange.org/).

This paper does not report original code.

Any additional information required to reanalyze the data reported in this paper is available from the lead contact upon request.

ACKNOWLEDGMENTS

The authors would like to thank Marie-Laure Martin for her help with statistics. C.C. is supported by the Marsden Fund Council from Government funding, managed by the Royal Society Te Apārangi (22-UOA-189). C.B. and O.K. are supported by the Swedish Foundation for Strategic Research (FFF20-0008). UPSC is supported by grants from the Knut and Alice Wallenberg Foundation and the Swedish Governmental Agency for Innovation Systems (VINNOVA).

AUTHOR CONTRIBUTIONS

F.B., E.H.M., and O.K. designed the project. C.B., M.S., C.C., E.H.M., O.K., and M.F. performed the experiments. C.B., E.H.M., M.S., and O.K. prepared

the figures. C.B., C.C., E.H.M., F.B., and O.K. wrote the manuscript. All authors have read and approved the final version.

DECLARATION OF INTERESTS

The authors declare no competing interests.

STAR★METHODS

Detailed methods are provided in the online version of this paper and include the following:

- KEY RESOURCES TABLE
- EXPERIMENTAL MODEL AND STUDY PARTICIPANT DETAILS
  - Plant material and growth conditions
- METHOD DETAILS
  - Mature pollen isolation and breaking
  - IMTACT procedures
  - SDS-PAGE immunoblot assay
  - Microscopy
  - Proteomic analysis
  - Transcriptomic analysis
  - Size distribution of the mitochondrial population in different tissues
  - LC/MS data analysis
  - GO network
- QUANTIFICATION AND STATISTICAL ANALYSIS

SUPPLEMENTAL INFORMATION

Supplemental information can be found online at https://doi.org/10.1016/j.cub.2024.12.037.

Received: June 7, 2024
Revised: October 17, 2024
Accepted: December 16, 2024
Published: January 28, 2025

REFERENCES

1. Benton, M.J., Wilf, P., and Sauquet, H. (2022). The Angiosperm Terrestrial Revolution and the origins of modern biodiversity. New Phytol. *233*, 2017–2035. https://doi.org/10.1111/nph.17822.
2. Borg, M., Brownfield, L., and Twell, D. (2009). Male gametophyte development: a molecular perspective. J. Exp. Bot. *60*, 1465–1478. https://doi.org/10.1093/jxb/ern355.
3. Hafidh, S., and Honys, D. (2021). Reproduction Multitasking: The Male Gametophyte. Annu. Rev. Plant Biol. *72*, 581–614. https://doi.org/10.1146/annurev-arplant-080620-021907.
4. Huang, J., Dong, J., and Qu, L.J. (2021). From birth to function: male gametophyte development in flowering plants. Curr. Opin. Plant Biol. *63*, 102118. https://doi.org/10.1016/j.pbi.2021.102118.
5. Kitazaki, K., Oda, K., Akazawa, A., and Iwahori, R. (2023). Molecular genetics of cytoplasmic male sterility and restorer-of-fertility for the fine tuning of pollen production in crops. Theor. Appl. Genet. *136*, 156. https://doi.org/10.1007/s00122-023-04398-8.
6. Møller, I.M., Rasmusson, A.G., and Van Aken, O. (2021). Plant mitochondria - past, present and future. Plant J. *108*, 912–959. https://doi.org/10.1111/tpj.15495.
7. Liu, J., Lim, S.L., Zhong, J.Y., and Lim, B.L. (2022). Bioenergetics of pollen tube growth in Arabidopsis thaliana revealed by ratiometric genetically encoded biosensors. Nat. Commun. *13*, 7822. https://doi.org/10.1038/s41467-022-35486-w.
8. Preuten, T., Cincu, E., Fuchs, J., Zoschke, R., Liere, K., and Börner, T. (2010). Fewer genes than organelles: extremely low and variable gene copy numbers in mitochondria of somatic plant cells. Plant J. *64*, 948–959. https://doi.org/10.1111/j.1365-313X.2010.04389.x.
9. Cai, Q., Guo, L., Shen, Z.R., Wang, D.Y., Zhang, Q., and Sodmergen. (2015). Elevation of Pollen Mitochondrial DNA Copy Number by WHIRLY2: Altered Respiration and Pollen Tube Growth in Arabidopsis. Plant Physiol. *169*, 660–673. https://doi.org/10.1104/pp.15.00437.
10. Lee, W., Zamudio-Ochoa, A., Buchel, G., Podlesniy, P., Marti Gutierrez, N., Puigròs, M., Calderon, A., Tang, H.Y., Li, L., Mikhalchenko, A., et al. (2023). Molecular basis for maternal inheritance of human mitochondrial DNA. Nat. Genet. *55*, 1632–1639. https://doi.org/10.1038/s41588-023-01505-9.
11. Nagata, N., Saito, C., Sakai, A., Kuroiwa, H., and Kuroiwa, T. (1999). The selective increase or decrease of organellar DNA in generative cells just after pollen mitosis one controls cytoplasmic inheritance. Planta *209*, 53–65. https://doi.org/10.1007/s004250050606.
12. Ma, F., Qi, H., Hu, Y.F., Jiang, Q.R., Zhang, L.G., Xue, P., Yang, F.Q., Wang, R., Ju, Y., Uchida, H., et al. (2018). The Mitochondrial Endonuclease M20 Participates in the Down-Regulation of Mitochondrial DNA in Pollen Cells. Plant Physiol. *178*, 1537–1550. https://doi.org/10.1104/pp.18.00754.
13. Matsushima, R., Tang, L.Y., Zhang, L., Yamada, H., Twell, D., and Sakamoto, W. (2011). A conserved, Mg(2)+-dependent exonuclease degrades organelle DNA during Arabidopsis pollen development. Plant Cell *23*, 1608–1624. https://doi.org/10.1105/tpc.111.084012.
14. Forner, J., Kleinschmidt, D., Meyer, E.H., Gremmels, J., Morbitzer, R., Lahaye, T., Schöttler, M.A., and Bock, R. (2023). Targeted knockout of a conserved plant mitochondrial gene by genome editing. Nat. Plants *9*, 1818–1831. https://doi.org/10.1038/s41477-023-01538-2.
15. Kuwabara, K., Arimura, S.I., Shirasawa, K., and Ariizumi, T. (2022). orf137 triggers cytoplasmic male sterility in tomato. Plant Physiol. *189*, 465–468. https://doi.org/10.1093/plphys/kiac082.
16. Li, W.Q., Zhang, X.Q., Xia, C., Deng, Y., and Ye, D. (2010). MALE GAMETOPHYTE DEFECTIVE 1, encoding the FAd subunit of mitochondrial F1F0-ATP synthase, is essential for pollen formation in Arabidopsis thaliana. Plant Cell Physiol. *51*, 923–935. https://doi.org/10.1093/pcp/pcq066.
17. Takatsuka, A., Kazama, T., Arimura, S.I., and Toriyama, K. (2022). TALEN-mediated depletion of the mitochondrial gene orf312 proves that it is a Tadukan-type cytoplasmic male sterility-causative gene in rice. Plant J. *110*, 994–1004. https://doi.org/10.1111/tpj.15715.
18. Grobei, M.A., Qeli, E., Brunner, E., Rehrauer, H., Zhang, R., Roschitzki, B., Basler, K., Ahrens, C.H., and Grossniklaus, U. (2009). Deterministic protein inference for shotgun proteomics data provides new insights into Arabidopsis pollen development and function. Genome Res. *19*, 1786–1800. https://doi.org/10.1101/gr.089060.108.
19. Klodová, B., Potěšil, D., Steinbachová, L., Michailidis, C., Lindner, A.C., Hackenberg, D., Becker, J.D., Zdráhal, Z., Twell, D., and Honys, D. (2023). Regulatory dynamics of gene expression in the developing male gametophyte of Arabidopsis. Plant Reprod. *36*, 213–241. https://doi.org/10.1007/s00497-022-00452-5.
20. Zhang, X., Liu, W., Nagae, T.T., Takeuchi, H., Zhang, H., Han, Z., Higashiyama, T., and Chai, J. (2017). Structural basis for receptor recognition of pollen tube attraction peptides. Nat. Commun. *8*, 1331. https://doi.org/10.1038/s41467-017-01323-8.
21. Rao, R.S., Salvato, F., Thal, B., Eubel, H., Thelen, J.J., and Møller, I.M. (2017). The proteome of higher plant mitochondria. Mitochondrion *33*, 22–37. https://doi.org/10.1016/j.mito.2016.07.002.
22. Boussardon, C., and Keech, O. (2022). Cell Type-Specific Isolation of Mitochondria in Arabidopsis. Methods Mol. Biol. *2363*, 13–23. https://doi.org/10.1007/978-1-0716-1653-6_2.
23. Boussardon, C., Przybyla-Toscano, J., Carrie, C., and Keech, O. (2020). Tissue-specific isolation of Arabidopsis/plant mitochondria - IMTACT (isolation of mitochondria tagged in specific cell types). Plant J. *103*, 459–473. https://doi.org/10.1111/tpj.14723.

24. Klepikova, A.V., Kasianov, A.S., Gerasimov, E.S., Logacheva, M.D., and Penin, A.A. (2016). A high resolution map of the Arabidopsis thaliana developmental transcriptome based on RNA-seq profiling. Plant J. *88*, 1058–1070. https://doi.org/10.1111/tpj.13312.

25. Dehaene, N., Boussardon, C., Andrey, P., Charif, D., Brandt, D., Gilouppe Taillefer, C., Nietzel, T., Ricou, A., Simon, M., Tran, J., et al. (2024). The mitochondrial orf117Sha gene desynchronizes pollen development and causes pollen abortion in the Arabidopsis Sha CMS. J. Exp. Bot. *75*, 4851–4872. https://doi.org/10.1093/jxb/erae214.

26. Honys, D., and Twell, D. (2004). Transcriptome analysis of haploid male gametophyte development in Arabidopsis. Genome Biol. *5*, R85. https://doi.org/10.1186/gb-2004-5-11-r85.

27. Olsen, O.A. (2001). Endosperm development: cellularization and cell fate specification. Annu. Rev. Plant Physiol. Plant Mol. Biol. *52*, 233–267. https://doi.org/10.1146/annurev.arplant.52.1.233.

28. Keech, O., Dizengremel, P., and Gardeström, P. (2005). Preparation of leaf mitochondria from Arabidopsis thaliana. Physiol. Plant. *124*, 403–409. https://doi.org/10.1111/j.1399-3054.2005.00521.x.

29. Hooper, C.M., Castleden, I.R., Tanz, S.K., Aryamanesh, N., and Millar, A.H. (2017). SUBA4: the interactive data analysis centre for Arabidopsis subcellular protein locations. Nucleic Acids Res. *45*, D1064–D1074. https://doi.org/10.1093/nar/gkw1041.

30. Shannon, P., Markiel, A., Ozier, O., Baliga, N.S., Wang, J.T., Ramage, D., Amin, N., Schwikowski, B., and Ideker, T. (2003). Cytoscape: a software environment for integrated models of biomolecular interaction networks. Genome Res. *13*, 2498–2504. https://doi.org/10.1101/gr.1239303.

31. Bindea, G., Mlecnik, B., Hackl, H., Charoentong, P., Tosolini, M., Kirilovsky, A., Fridman, W.H., Pagès, F., Trajanoski, Z., and Galon, J. (2009). ClueGO: a Cytoscape plug-in to decipher functionally grouped gene ontology and pathway annotation networks. Bioinformatics *25*, 1091–1093. https://doi.org/10.1093/bioinformatics/btp101.

32. Thimm, O., Bläsing, O., Gibon, Y., Nagel, A., Meyer, S., Krüger, P., Selbig, J., Müller, L.A., Rhee, S.Y., and Stitt, M. (2004). MAPMAN: a user-driven tool to display genomics data sets onto diagrams of metabolic pathways and other biological processes. Plant J. *37*, 914–939. https://doi.org/10.1111/j.1365-313x.2004.02016.x.

33. Nelson, C.J., Li, L., Jacoby, R.P., and Millar, A.H. (2013). Degradation rate of mitochondrial proteins in Arabidopsis thaliana cells. J. Proteome Res. *12*, 3449–3459. https://doi.org/10.1021/pr400304r.

34. Edlund, A.F., Olsen, K., Mendoza, C., Wang, J., Buckley, T., Nguyen, M., Callahan, B., and Owen, H.A. (2017). Pollen wall degradation in the Brassicaceae permits cell emergence after pollination. Am. J. Bot. *104*, 1266–1273. https://doi.org/10.3732/ajb.1700201.

35. Lee, S.L.J., and Warmke, H.E. (1979). Organelle Size and Number in Fertile and T-Cytoplasmic Male-Sterile Corn. Am. J. Bot. *66*, 141–148. https://doi.org/10.1002/j.1537-2197.1979.tb06206.x.

36. Firon, N., Nepi, M., and Pacini, E. (2012). Water status and associated processes mark critical stages in pollen development and functioning. Ann. Bot. *109*, 1201–1214. https://doi.org/10.1093/aob/mcs070.

37. Colaço, R., Moreno, N., and Feijó, J.A. (2012). On the fast lane: mitochondria structure, dynamics and function in growing pollen tubes. J. Microsc. *247*, 106–118. https://doi.org/10.1111/j.1365-2818.2012.03628.x.

38. Selinski, J., and Scheibe, R. (2014). Pollen tube growth: where does the energy come from? Plant Signal. Behav. *9*, e977200. https://doi.org/10.4161/15592324.2014.977200.

39. Petereit, J., Duncan, O., Murcha, M.W., Fenske, R., Cincu, E., Cahn, J., Pružinská, A., Ivanova, A., Kollipara, L., Wortelkamp, S., et al. (2020). Mitochondrial CLPP2 Assists Coordination and Homeostasis of Respiratory Complexes. Plant Physiol. *184*, 148–164. https://doi.org/10.1104/pp.20.00136.

40. Steinhorst, L., and Kudla, J. (2013). Calcium - a central regulator of pollen germination and tube growth. Biochim. Biophys. Acta *1833*, 1573–1581. https://doi.org/10.1016/j.bbamcr.2012.10.009.

41. Zheng, R.H., Su, S.D., Xiao, H., and Tian, H.Q. (2019). Calcium: A Critical Factor in Pollen Germination and Tube Elongation. Int. J. Mol. Sci. *20*, 420. https://doi.org/10.3390/ijms20020420.

42. Selles, B., Michaud, C., Xiong, T.C., Leblanc, O., and Ingouff, M. (2018). Arabidopsis pollen tube germination and growth depend on the mitochondrial calcium uniporter complex. New Phytol. *219*, 58–65. https://doi.org/10.1111/nph.15189.

43. Wagner, S., Behera, S., De Bortoli, S., Logan, D.C., Fuchs, P., Carraretto, L., Teardo, E., Cendron, L., Nietzel, T., Füßl, M., et al. (2015). The EF-Hand Ca2+ Binding Protein MICU Choreographs Mitochondrial Ca2+ Dynamics in Arabidopsis. Plant Cell *27*, 3190–3212. https://doi.org/10.1105/tpc.15.00509.

44. Wang, M., and Teng, Y. (2018). Genome-wide identification and analysis of MICU genes in land plants and their potential role in calcium stress. Gene *670*, 174–181. https://doi.org/10.1016/j.gene.2018.05.102.

45. Gutiérrez-Mireles, E.R., Páez-Franco, J.C., Rodríguez-Ruíz, R., Germán-Acacio, J.M., López-Aquino, M.C., and Gutiérrez-Aguilar, M. (2023). An Arabidopsis mutant line lacking the mitochondrial calcium transport regulator MICU shows an altered metabolite profile. Plant Signal. Behav. *18*, 2271799. https://doi.org/10.1080/15592324.2023.2271799.

46. Wang, Y., Han, Y., She, J., Nguyen, N.X., Mootha, V.K., Bai, X.C., and Jiang, Y.X. (2020). Structural insights into the Ca2+ -dependent gating of the human mitochondrial calcium uniporter. eLife *9*, e60513. https://doi.org/10.7554/eLife.60513.

47. Denton, R.M., Rutter, G.A., Midgley, P.J.W., and Mccormack, J.G. (1988). Effects of Ca-2+ on the Activities of the Calcium-Sensitive Dehydrogenases within the Mitochondria of Mammalian-Tissues. J. Cardiovasc. Pharmacol. *12*, S69–S72.

48. Yamaoka, S., and Leaver, C.J. (2008). EMB2473/MIRO1, an Miro GTPase, is required for embryogenesis and influences mitochondrial morphology in pollen. Plant Cell *20*, 589–601. https://doi.org/10.1105/tpc.107.055756.

49. Diao, M., Qu, X., and Huang, S. (2018). Calcium imaging in Arabidopsis pollen cells using G-CaMP5. J. Integr. Plant Biol. *60*, 897–906. https://doi.org/10.1111/jipb.12642.

50. Twell, D., Yamaguchi, J., and McCormick, S. (1990). Pollen-specific gene expression in transgenic plants: coordinate regulation of two different tomato gene promoters during microsporogenesis. Development *109*, 705–713. https://doi.org/10.1242/dev.109.3.705.

51. Gerola, P.D., Mol, C.A., Newbigin, E., and Lush, W.M. (2000). Regulation of LAT52 promoter activity during pollen tube growth through the pistil of Nicotiana alata. Sex. Plant Reprod. *12*, 347–352. https://doi.org/10.1007/s004970000022.

52. Zheng, H., Bednarek, S.Y., Sanderfoot, A.A., Alonso, J., Ecker, J.R., and Raikhel, N.V. (2002). NPSN11 is a cell plate-associated SNARE protein that interacts with the syntaxin KNOLLE. Plant Physiol. *129*, 530–539. https://doi.org/10.1104/pp.003970.

53. Schneider, C.A., Rasband, W.S., and Eliceiri, K.W. (2012). NIH Image to ImageJ: 25 years of image analysis. Nat. Methods *9*, 671–675. https://doi.org/10.1038/nmeth.2089.

54. Cox, J., and Mann, M. (2008). MaxQuant enables high peptide identification rates, individualized p.p.b.-range mass accuracies and proteome-wide protein quantification. Nat. Biotechnol. *26*, 1367–1372. https://doi.org/10.1038/nbt.1511.

55. Tyanova, S., Temu, T., Sinitcyn, P., Carlson, A., Hein, M.Y., Geiger, T., Mann, M., and Cox, J. (2016). The Perseus computational platform for comprehensive analysis of (prote)omics data. Nat. Methods *13*, 731–740. https://doi.org/10.1038/nmeth.3901.

56. R Core Team (2021). R: A Language and Environment for Statistical Computing.

57. Perez-Riverol, Y. (2022). Proteomic repository data submission, dissemination, and reuse: key messages. Expert Rev. Proteomics *19*, 297–310. https://doi.org/10.1080/14789450.2022.2160324.

STAR★METHODS

KEY RESOURCES TABLE

REAGENT or RESOURCE	SOURCE	IDENTIFIER
Antibodies		
Rabbit polyclonal anti-IDH	Agrisera	AS06 203A
Rabbit polyclonal anti-VDAC	Agrisera	AS07 212
Rabbit polyclonal anti-TOC34	Agrisera	AS07 238
Rabbit polyclonal anti-LHCB1	Agrisera	AS01 004
Rabbit polyclonal anti-UGPase	Agrisera	AS05 086
Rabbit polyclonal anti-HIS3	Agrisera	AS10 710
Rabbit polyclonal anti-CAT	Agrisera	AS09 501
Rabbit polyclonal anti-SEC12	Zheng et al.[52]	N/A
Goat anti-rabbit secondary antibody conjugated to HRP	Agrisera	AS09 602
Chemicals, peptides, and recombinant proteins		
Na4P2O7	Merck	106591; CAS: 7722-88-5
PVP40	Sigma-Aldrich	PVP40-1KG; CAS: 9003-39-8
BSA	Sigma-Aldrich	A9647; CAS: 9048-46-8
L-Cysteine	Sigma-Aldrich	168149-25G; CAS: 52-90-4
Sodium ascorbate	Sigma-Aldrich	11140-50G; CAS: 134-03-2
TES	Sigma-Aldrich	T1375-100G; CAS: 7365-44-8
Glycerol	Sigma-Aldrich	G5516-1L; CAS: 56-81-5
Triton X-100	Sigma-Aldrich	X100–1L; CAS: 9036-19-5
Protein Assay Dye Reagent Concentrate	Bio-Rad	500-006; CAS: 7664-38-2 and 67-56-1
Acetone	VWR	20063.365; CAS: 67-64-1
DTT	Sigma-Aldrich	10708984001; CAS: 3483-12-3
Bromophenol blue	Sigma-Aldrich	B0126; CAS: 115-39-9
ECL kit bright	Agrisera	AS16 ECL-N-100
Mitotracker Orange CMTMRos	ThermoFischer	M7510; CAS: 199116-50-2
Urea	VWR	28877.292; CAS: 57-13-6
Thiourea	Sigma-Aldrich	T8656; CAS: 62-56-6
Iodoacetamide	Sigma-Aldrich	I6125; CAS: 144-48-9
Trypsin/LysC	Promega	V5071; CAS: 9002-07-7
TFA	Sigma-Aldrich	T6508; CAS: 76-05-1
Acetonitrile	Sigma-Aldrich	34851; CAS: 75-05-08
Formic acid	Sigma-Aldrich	F0507; CAS: 64-18-6
Deposited data		
Mass spectrometry proteomics data	This paper	PXD050553 https://www.proteomexchange.org/
Experimental models: Organisms/strains		
Arabidopsis: UBQ10::OM64-eGFP-BLRP and UBQ10::BirA expression cassettes (T3)	Boussardon et al.[23]	https://onlinelibrary.wiley.com/doi/full/10.1111/tpj.14723
Software and Algorithms		
ImageJ	Schneider et al.[53]	https://imagej.net/ij/
MaxQuant 2.1.3.0	Cox and Mann[54]	https://www.maxquant.org/
Perseus 1.6.15.0	Tyanova et al.[55]	https://www.maxquant.org/perseus/
R	R Core Team[56]	https://www.r-project.org/

(*Continued on next page*)

Continued

REAGENT or RESOURCE	SOURCE	IDENTIFIER
SUBA5	Hooper et al.[29]	https://suba.live/
Cytoscape	Shannon et al.[30]	https://cytoscape.org/
ClueGO	Bindea et al.[31]	https://apps.cytoscape.org/apps/cluego
MapMan	Thimm et al.[32]	https://mapman.gabipd.org/mapman
ImageJ	BioRender	https://www.biorender.com/
Other		
Glass beads	Sigma-Aldrich	G8772-100G
Retsch MM400 mixer mill	Retsch	https://www.retsch.com/products/milling/ball-mills/mixer-mill-mm-400/
Dynabead MyOne Streptavidin T1	ThermoFischer	65601
Azure c600 Western Blot Imaging system	Azure biosystems	AZI600-01
ZipTips with C18 resin	Millipore	ZTC18S096
ACQUITY UPLC M-Class Peptide BEH C18 Column	Waters	186007484
PicoTip Emitter; 360 μm OD × 20 μm ID, 10 μm tip; 12 cm L	Coanntech	TIP36002005−12
LSM780 confocal microscope	Zeiss	N/A
Orbitrap Exploris 480	ThermoFischer	https://assets.thermofisher.com/TFS-Assets/CMD/brochures/br-65448-ms-orbitrap-exploris-480-br65448-en.pdf
Dionex UltiMate 3000 RSLCnano system	ThermoFischer	174500
Carl Zeiss MERLIN Field Emission Scanning Electron Microscope	Carl Zeiss	N/A
Energy dispersive X-ray spectrometer	Oxford Instruments	EDS X-max

EXPERIMENTAL MODEL AND STUDY PARTICIPANT DETAILS

Plant material and growth conditions

Arabidopsis thaliana Columbia-0 (Col-0) T3 homozygous plants containing the *UBQ10::OM64-eGFP-BLRP* and *UBQ10::BirA* expression cassettes described in Boussardon et al.[23] were grown under long-day photoperiod (LD: light 16 h at 22°C, dark 8 h at 17°C) at 65% relative humidity and 150 μmol m^{-2} s^{-1} photosynthetically active radiation (PAR) or short-day photoperiod (SD: light 8 h at 22°C, dark 16 h at 17°C) at 65% relative humidity and 180 μmol m^{-2} s^{-1} PAR on a mixture soil:vermiculite 3:1.

Seeds were systematically sterilized by 70% ethanol for 10 min, followed by 10 min in 56% (v/v) ethanol. Once ethanol was discarded, seeds were air-dried for 1 h and stratified at 4°C in 0.1% agarose for 3 days.

METHOD DETAILS

Mature pollen isolation and breaking

We used 7-week-old plants. In our conditions, this corresponded to the flowering stage with branching on the main stem and flowered secondary stems. All steps were done on ice with pre-cooled material. We manually collected inflorescences and distributed them in two 50 ml tubes. By using around 20 plants, we got around 6 g of fresh material for each biological replicate (two collection tubes). We added 10 ml/g FW of grinding buffer (0.3 M sucrose, 25 mM $Na_4P_2O_7$, 10 mM KH_2PO_4, 20 mM PVP40, 0.3% [w/v] BSA, 20 mM sodium ascorbate and 10 mM L cysteine, pH adjusted to 8.0 with KOH). Tubes were shaken vigorously by hand for 1 min to release mature pollen. The mixture was filtered through an 80 μm mesh stainless steel sieve. This step was repeated twice. The pollen suspension was filtered through a 40 μm mesh stainless steel and the pollen concentration was estimated by counting an aliquot in a Malassez counting chamber. Mature pollen grains were collected by a centrifugation step at 900 *g*, 10 min at 4°C in a swinging rotor and the pellet was resuspended in a volume of grinding buffer to obtain a concentration of 10^6 pollen grains/ml. The pollen suspension was distributed into 1 ml aliquots into as many as necessary 1.5 ml eppendorf tubes previously filled with 0.5 g of glass beads (Sigma, G8772-100G glass beads acid washed). Pollen grains were broken by shaking the tubes for 3 min (180 s) at 30 Hz in a Retsch MM400 mixer mill. The bead-free sample was collected in a new tube by making a small hole at the bottom of the tube and centrifuging for 5 min, 900 *g*, 4°C. The beads were rinsed once with 1 ml of grinding buffer and centrifuged again in the same collecting tube. All recovered samples were pooled into a 50 ml tube and the efficiency of the breakage was checked on an aliquot under the microscope. At this stage, we added 1 volume of new buffer (0.3 M sucrose, 25 mM $Na_4P_2O_7$, 10 mM KH_2PO_4, 60 mM TES, 10 mM EDTA, 1 mM glycine, 90 mM PVP40, 1% [m/v] BSA, 50 mM sodium ascorbate and 20 mM cysteine L, pH adjusted to 8.0 with KOH). After

gentle mixing, and centrifugation for 10 min, 900 *g*, 4°C, the supernatant was carefully transferred to a new tube. An organelle-enriched pellet containing mitochondria was obtained by centrifuging the sample for 15 min, 15,000 *g*, + 4°C. This pellet was directly used in the IMTACT procedure.

IMTACT procedures

All steps were performed in a cold room (at 4°C) and on ice with pre-cooled materials.

For sporophytic tissues, floral buds (i.e. 0.3 g of floral buds) from 7-week-old plants were harvested and transferred to a mortar. Protocol was performed as described in Boussardon and Keech[22] and Boussardon et al.[23] on 1 μm magnetic beads (ThermoFischer, Dynabead MyOne Streptavidin T1, 65601). For pollen extracts, the pellet obtained from the last centrifugation step after breaking the pollen was homogenised in 4 ml of either Keech's grinding buffer (2 mM EDTA, 10 mM TES, 10 mM KH_2PO_4, 0.3 M sucrose and pH adjusted with KOH to 7.5) or KPBS buffer (136 mM KCl, 10 mM KH_2PO_4, pH adjusted with KOH to 7.25). A small volume (aproximately 100 μl) of crude extract was aliquoted for further analysis. 50 μl of 1 μm washed beads were added to the crude extract and tubes were incubated on a rotating wheel for 5 min at 10 rpm. The beads were separated using a magnet for 2 min and the supernatant was discarded. The beads were washed 5 times using 600, 500, 400, 300 and 200 μl of Keech's wash buffer, respectively, and were finally resuspended in 100 μl wash buffer. Bead-bound mitochondria were lysed with 2 volumes of mitochondria lysis buffer (50 mM TES/KOH pH 7.5, 2 mM EDTA, 5 mM $MgCl_2$, 10% [v/v] glycerol, and 0.1% [v/v] Triton X-100). Beads were separated and the supernatant was conserved. Protein concentration was obtained by Bradford assay using the microassay procedure (Bio-Rad, Protein Assay Dye Reagent Concentrate, 500-006). Proteins were mixed with 4 volumes of acetone (stored at -20°C) and precipitated for 1 hour at -20°C. Proteins were pelleted at 13000 *g* for 10 min at room temperature. Acetone was discarded and pellet was air-dried for 20 min (no more than 30 min) at room temperature.

SDS-PAGE immunoblot assay

For immunoblot analysis, crude extracts and pelleted isolated mitochondria proteins were mixed with 2X Laemmli sampling buffer (4% SDS, 20% glycerol, 0.125 M Tris-HCl pH 6.8, and 0.005% bromophenol blue) supplemented with 0.2 M DTT and incubated at 95°C for 10 min before separating the protein mixtures on reducing 12% polyacrylamide gel.

After migration at 110 V, proteins were transferred during 1 h at 270 mA onto a 0.45 μm nitrocellulose membrane. Membranes were blocked with 5% milk in TBS-T for 1h followed by an overnight incubation at 4°C with specific polyclonal primary antibodies raised against the mitochondrial isocitrate dehydrogenase protein (IDH; 39 kDa; 1/1000, Agrisera, AS06 203A), the mitochondrial voltage-dependent anion-selective channel protein 1-5 (VDAC; 29 kDa; 1/1000, Agrisera, AS07 212), the chloroplastic translocon of the outer envelope membrane of chloroplasts 34 protein for pollen (TOC34; 27 kDa; 1/10000, Agrisera, AS07 238), the chloroplastic LHCII type I chlorophyll a/b-binding protein for floral buds (LHCB1; 25 kDa; 1/1000, Agrisera, AS01 004), the cytosolic UDP-glucose pyrophosphorylase (UGPase; 51.6 kDa; 1/1000, Agrisera, AS05 086), the nuclear histone 3 (HIS3; 15 kDa; 1/5000, Agrisera, AS10 710), and the peroxisomal catalase (CAT; 55 kDa; 1/1000, Agrisera, AS09 501) or the endoplasmic reticulum protein SEC12 (40 kDa; 1/3000; Zheng et al.[52]) diluted in 2 % milk in TBS-T. After 1 h incubation at room temperature with a goat anti-rabbit secondary antibody conjugated to horseradish peroxidase (1/15000 in 2 % milk in TBS-T, Agrisera, AS09 602), visualization was carried out using a chemiluminescence kit (Agrisera ECL kit bright; AS16 ECL-N-100) and signals were detected using Azure c600 Western Blot Imaging system (Azure biosystems). Exposure time were 30 s (standard sensitivity). Of note, in our hands, the buffer used in Keech et al.[28] gave the best results in terms of contaminants and mitochondria matrix/OMM ratio (Figure S4).

Microscopy

Confocal imaging

Floral buds from 7-week-old WT and IMTACT plants grown in LD were vacuum infiltrated with 100 nM of Mitotracker Orange CMTMRos (ThermoFischer, M7510), diluted in ½ MS, for 5 min and incubated 15 min in darkness. Mature pollen was dispersed in ½ MS supplemented 100 nM mitotracker and incubated at room temperature for 10 min. Samples were observed on a confocal microscope (Zeiss, LSM780) and a Zeiss Zen software (40X, water immersion). Signals were detected using the excitation/emission wavelengths: eGFP (488 nm/495-535 nm), Mitotracker (561 nm/575-630 nm). Pictures were analysed using the ImageJ software (https://imagej.nih.gov/ij/).[53]

Scanning Electron Microscopy

For SEM, mitochondria coupled to beads were fixed, dispersed and sedimented onto glass coverslips, subsequently dehydrated in a series of graded ethanol, critical point dried and coated with 2 nm iridium. The morphology of samples was analysed by field-emission scanning electron microscopy (FESEM; Carl Zeiss Merlin) using secondary electron detector at accelerating voltage of 2-4 kV and probe current of 100 pA. Elemental distribution was performed using energy dispersive X-ray spectrometer (EDS; Oxford Instruments X-Max 80 mm2) at accelerating voltage of 10 kV and probe current of 300 pA.

Proteomic analysis

Protein digestion

Proteins from crude and IMTACT samples (between 4 and 15 μg of protein per sample) were dissolved in solubilization buffer (6 M urea/2 M thiourea pH 8.0) to adjust the protein concentration to 0.5 μg/μl. Proteins were reduced by incubation for 30 min at 22°C with DTT (1 μg per 10 μg protein) and then alkylated by incubation for 20 min at 22°C in the dark with iodoacetamide (5 μg per 10 μg

protein). Samples were diluted four times with 10 mM Tris-HCl pH 8.0 and the proteins were digested for 15 h at 37°C using a Trypsin/LysC mixture (Promega, 0.4 μg protease per 10 μg protein). The samples were acidified to 0.2 % (v/v) TFA and centrifuged at 14 000 g for 10 minutes to eliminate any insoluble material. The peptides present in the supernatant were purified using ZipTips with C18 resin (Millipore) according to the manufacturer instructions and dried down.

MS analysis

The peptides were resuspended in 3 % (v/v) acetonitrile, 0.1 % (v/v) formic acid and 150 ng of digested peptides were separated on a Dionex UltiMate 3000 RSLCnano system consisting of a NCS-3500RS Nano ProFlow and WPS-3000TPL RS UPLC System (ThermoFischer, Dreieich, Germany) equipped with a PepMap™ Neo 5 μm C18 300 μm × 5 mm Trap cassette (ThermoFischer, Dreieich, Germany, https://www.thermofisher.com/order/catalog/product/de/de/174500) as well as a ACQUITY UPLC M-Class Peptide BEH C18 Column, 130Å, 1.7 μm, 75 μm × 250 mm (Waters, Eschborn, Germany, https://www.waters.com/nextgen/de/de/shop/columns/186007484-acquity-uplc-m-class-peptide-beh-c18-column-130a-17–m-75–m-x-2.html). After peptides were trapped for 10 min at 15 μl/min at 3% solvent B (solvent A: 0.1% (v/v) formic acid in water, solvent B: 0.1% (v/v) formic acid in ACN) and separated at 240 nl/min with a linear gradient of 3-50% B within 50 min. Eluting peptides were ionized at 2.1 kV and 320 °C in a Exploris 480 ThermoFischer nanoESI source using a Pre-cut PicoTip Emitter; 360 μm OD × 20 μm ID, 10 μm tip; 12 cm long (CoAnn Technologies, LLC). The Exploris 480 was equipped with a FAIMS device. The settings used were: CV of-50 V, MS range of 350–1500 m/z, 1 s cycle time, 120000 Orbitrap resolution, with a normalized AGC target of 300%, and minimum IT of 50 ms. Centroided MSMS of each selected precursor were collected at normalized HCD of 31% and a resolution of 15000, an AGC target of 100% and IT of 35 ms. Each precursor was then excluded from analysis for 30 s after one hit. The mass spectrometry proteomics data have been deposited to the ProteomeXchange Consortium via the PRIDE[57] partner repository with the dataset identifier PXD050553.

Transcriptomic analysis

Data, accession code E-MTAB-9456 (ArrayExpress), were downloaded from Klodová et al.[19] (Supplementary File 1 "TPM values for RNA-seq samples of Col-0 and Ler-0 with AGI identifiers"). For each transcript, its expression value was normalized to the highest value within the four stages, and then replicates for each developmental stage were averaged.

Size distribution of the mitochondrial population in different tissues

Scanning electron microscopy pictures were used to estimate the distribution of the size of mitochondria in different tissues, i.e. mesophyll, vascular and pollen. As mitochondria were spherical, diameter in nm was quantified using the ImageJ software.[53] Size distribution (in percentage; with standard deviation) of the mitochondrial population isolated from mesophyll (4 replicates, n=176), vascular (6 replicates, n=258) and pollen (4 replicates, n=70) cells. Mitochondrial size distribution for mesophyll and vascular cells were retrieved from Boussardon et al.[23] Related to Figure 2B.

LC/MS data analysis

Data analysis

Acquired LC-MS/MS spectra were queried against an in-house modified Araport11 database including all nuclear encoded proteins as well as protein models of the mitochondrial and plastid genomes after RNA editing using MaxQuant 2.1.3.0.[54] Default parameters were used, and the protein quantification function was selected. The output proteingroup file was then imported into Perseus 1.6.15.0[55] and the LFQ values were used for calculations. They were first $\log_2$ transformed and filtered to keep proteins that were identified in at least 3 replicates of one of the four samples.

The SUBA5 website was used to identify the cellular localization of proteins[29] (https://suba.live/).

The consistency between biological repeats was assessed by hierarchical clustering (Euclidian distance, Ward's method) using the hclust function in R version 3.6.3 (2020-02-29)[56] on Data S1A.

Principal Component Analysis (PCA) graphs were generated on R (v.2023.09.1+494) on Data S1A and S4 A.S

We identified differentially abundant proteins (DAP) between pollen and bud mitochondria by performing Student's t-test (two-tailed; FDR: 0.05) on IP versus IB samples with a q-value threshold = 0.05. If data were taken as such and corrected with a FDR (0.05), only 19 mitochondrial proteins would appear as differentially abundant in crude and 120 in IMTACT extracts. Since such approach compromised the biological relevance of the comparison between tissues, we decided to first pre-filter our data through a present/absent step, in which protein groups not identified in 4 replicates in a tissue were labelled as "absent". A Student's t-test with a FDR correction (at 0.05) was applied to the present datatset (Data S4A; Figure S8).

GO network

A biological network was built using the Cytoscape (version 3.10.1) with the compatible plug-in ClueGO (version 2.5.10). GO terms (Biological Process) from significantly ($p < 0.05$) pDAP in mitochondria from mature pollen versus mitochondria from floral buds. Only one gene model was used for GO terms. Enriched GO terms upregulated in mitochondrial proteomes from mature pollen (palette of pink) or downregulated (palette of gold) were clustered according to their functional categories. The reference used for ontology was the file: GO_BiologicalProcess-Custom-GOA-ACAP-ARAP_12.02.2024. EnsemblGeneID, EntrezGeneID and SymbolID were used as identifiers. The following parameters were applied to generate the networks: min GO level = 2, max GO level = 10, number of "proteins" per term = 2, and 4.0% "proteins" per term for all clusters; the minimum percentage for a cluster to be significant was 60%,

both GO fusion and GO group were applied, Kappa score was fixed at 0.4, with an initial group size of 1 and a sharing group percentage set at 50%. The statistical test used for enrichment/ depletion was a two-sided hypergeometric test with a Bonferroni step down correction method applied. The size of a node is proportional to the number of proteins contributing to this node, while the intensity of the colour is proportional to the significance of it (the minimum for significance being $p < 0.05$); grey nodes = over-represented in the protein subset but not enriched significantly; the threshold of significance was set at 60%. Related to Figure 3A.

Metabolic pathways of the dataset were obtained from MapMan (v. 3.6.0RC1). Bins were isolated from the TAIR10 *Arabidopsis thaliana* genome (Ath_AGI_LOCUS_TAIR10_Aug2012.m02). Related to Figure 3B.

QUANTIFICATION AND STATISTICAL ANALYSIS

The precise statistics for each figure can be found in the method details section above as well as in the respective figure's caption.